ELSEVIER

Polymer 42 (2001) 6641–6650

polymer

www.elsevier.nl/locate/polymer

Are microcomposites realistic models of the fibre/matrix interface? II. Physico-chemical approach

P. Zinck[a], H.D. Wagner[b], L. Salmon[c], J.F. Gerard[a,*]

[a]*Laboratoire des Matériaux Macromoléculaires, LMM UMR 5637 CNRS, Institut National des Sciences Appliquées de Lyon, Bâtiment 403, 69621 Villeurbanne Cedex, France*

[b]*Department of Materials and Interfaces, The Weizmann Institute of Science, Rehovot 76100, Israel*

[c]*EMA, DER, Centre de Recherche EDF des Renardières, 77250 Moret-sur Loing, France*

Received 21 June 2000; received in revised form 25 October 2000; accepted 24 November 2000

Abstract

The physical and mechanical properties of microdroplets can differ significantly from those of the bulk material. This is especially true for epoxyde droplets, owing to (i) diffusion and vaporization of the hardener during the first step of the cure, (ii) surface oxidation and (iii) possible hydrolysis of the hardener during the first step of the cure schedule. The glass transition temperature of microdroplets was found to be 20–50°C lower than that of the bulk material. It is shown that this leads to microdroplets exhibiting a higher Young's modulus and a lower yield point than the bulk network. Those discrepancies influence the adhesion between fibre and matrix by changing the stress distribution at the interface and can lead to biased results when comparing different matrices with the microbond test. The general idea that microbond specimens behave like ideal elastic components is now reassessed in view of (i) a plastic flow of the polymeric droplet and (ii) the occurrence of rate-dependent processes. This leads to a fundamental question regarding the use of microcomposites as a model of macroscopic-scale specimens.

Keywords: Microbond test; Interphase; Adhesion

1. Introduction

The fibre–matrix interphase properties of fibre reinforced polymer composites can be characterized through micromechanical testing, such as pull-out [1], microbond test [2], fragmentation [3] and micro-indentation [4]. In spite of the apparent simplicity of microcomposites, micromechanical analysis of the results is usually required in order to obtain informations on the interfacial properties. Research in the area of fibre pull-out has considered the fracture mechanisms of fibre matrix failure [5], leading to numerous theoretical models. The microbond test developed by Miller et al. [6] has been used widely in the literature devoted to the adhesion between various types of polymer and fibres. In fact, its main advantage is its simplicity as compared to the pull-out configuration. Both tests are now considered as a mode I or mixed mode failure test of the interface [7,8]. They do not provide a true interfacial shear strength (IFSS), and as a consequence, an energy balance approach must be used for fitting the experimental data. Among the numerous models proposed in the literature, it seems preferable to use those considering fracture initiation for the microbond test [9] such as the approach of Scheer and Nairn [7]. It is also the only model which considers the specific microbond geometry. One limiting aspect of theoretical modelling was revealed by the observation of a plastic flow of the polymeric droplet [9,10], leading to a re-evaluation of the hypothesis of ideal elasticity assumed in all models. Polymers are indeed known to behave like viscoelastic bodies. Besides, it was also shown in the case of an epoxyde matrix that a microdroplet could exhibit properties different from those of the bulk material, and in particular a lower glass transition temperature owing to a deviation from the stoichiometry [11] as a consequence of the cure schedule. This leads to some important consequences and questions:

- Is a microcomposite representative of the macroscopic scale?
- Can the results of the microbond test be biased through
  - energy dissipation due to the plastic flow?
  - differences in physical and mechanical properties of the microdroplet?
- Can processing conditions affect the measurement of interfacial adhesion ?

* Corresponding author.

0032-3861/01/$ - see front matter
PII: S0032-3861(00)00871-5

The aim of this paper is to answer these questions, and in particular:

(1) to show in the case of epoxyde matrices that microdroplets exhibit properties different from those of the bulk material and to evaluate those differences;
(2) to highlight the visco-elastic and plastic behaviour of the specimens;
(3) to characterize the consequences of those considerations on the interfacial adhesion as measured by the microbond technique.

2. Microdroplet processing parameters and their influence on adhesion measurement

The aim of this section is to heighten the reader's awareness to the importance of processing conditions, i.e. to show that for the same system, the results provided by the microbond test are influenced strongly by the procedure used to make the droplet.

We will begin this part by a brief discussion on the influence of the cure schedule of thermosets. This involves mainly two parameters: (i) the degree of cross-linking and (ii) the residual stresses resulting from thermal shrinkage. Biro et al. [12] showed using a diglycidyl ether of bisphenol A (DGEBA)/aromatic diamine/carbon fibre system that the higher the cross-link density, the higher the IFSS obtained. It is thus necessary to control this parameter. When a microbond test is performed in an attempt to compare different thermosetting matrices, one has to determine a cure schedule which leads to a fully cross-linked system since it is difficult to obtain similar 'under-cured' states. The residual shrinking stresses are also related to the cure schedule, since they are proportional to the difference between the glass transition temperature and the room temperature. This parameter is of great importance when comparing two matrices that exhibit different glass transition temperatures. Results taken from Ref. [12] are shown in Table 1 for a matrix with a glass transition temperature of 161°C. It should be noticed that the value of the average IFSS can vary by more than 100% on the same system merely as a consequence of the cure schedule.

Table 1
Effect of the cure schedule of an epoxy network on the average IFSS measured with the microbond technique. After Biro et al. [12]

Pre-cure	Cure	Post-cure	τ (MPa)
2 h, 60°C	2 h, 120°C	–	30 ± 9
2 h, 60°C	2 h, 120°C	2 h, 165°C	58 ± 13
2 h, 60°C	1 h, 120°C	5 h, 180°C	67 ± 11

In the case of semi-crystalline polymers, the temperature of deposition of the droplet as well as the cooling rate can also influence the interfacial adhesion obtained via the crystallinity of the matrix. Results taken from previous work [10] are presented in Table 2. Again, the value of the IFSS can vary by 50% on the same system by varying the procedure to deposit the droplet.

Varying the specific geometry of the microdroplet, i.e. the surface/volume ratio, can lead to a material different from the bulk matrix. This aspect was emphasized on a DGEBA/diamine aromatic system [11]. It was shown that the diffusion of the rather volatile *m*-PDA hardener at early stages of the cure leads to low values of the IFSS. The glass transition temperature of small droplets (<150 μm) was found to be 60°C lower than that of the bulk material. This was not the case with the less volatile J-700 polyetheramine. The method to alleviate the diffusion problem is a pre-cure at room temperature, which enables the epoxyde–amine reaction to begin. It is important to know whether this phenomenon is general in epoxyde systems, or specific to the volatile *m*-PDA hardener. The use of thin films as ideal microdroplet model is proposed hereafter, as a complement of adhesion measurements.

3. Experimental section

3.1. Materials

E-glass fibres were supplied by VETROTEX Int. Their sizing is referred to as P122 by Vetrotex Co., known as a 'universal sizing', i.e. suitable for epoxyde as well as polyester matrices. The coupling agent included in this sizing formulation was γ-aminopropyltriethoxysilane (γ-APS) (denoted A1100) from a 1-wt% aqueous solution of silane. Other constituents such as a lubricant and a film former were also included.

The diameter was measured by optical microscopy with a sample size of 100. Results are given in Table 3 together with mechanical properties. The amount of sizing (by

Table 2
Evolution of the IFSS with the crystallinity of the poly(phenylene sulfide)/glass fibre interface. After Gonon et al. [10]

Procedure to deposit the droplet	IFSS (MPa)	DSC analysis	
		Heat of fusion (cal/g)	Crystallinity (%)
15 min at 330°C slow cooling at 1°C/min	33	9.5	50
30 min at 330°C annealing 30 min at 200°C	22	6.6	35

Table 3
Mechanical and thermal properties of the E-glass fibres

Tensile modulus (GPa)	73
Poisson coefficient	0.22
Thermal expansion factor (K^{-1})	5×10^{-6}
Diameter (μm)	19.1 ± 1.4
Weight loss[a] (wt%)	0.77
Sizing thickness[b] (nm)	86
Average tensile strength at 20 mm (GPa)	1.75

[a] Determined from TGA analysis.
[b] Calculated assuming a continuous layer.

weight) was determined by thermogravimetric analysis under inert atmosphere (heating rate: 5 K min^{-1}) and the thickness of the deposit layer was estimated assuming a continuous layer.

Matrices considered in this study are polyepoxies based on DGEBA. Two different hardeners were selected: 4,4′ methylenebis2,6-diethyleneaniline (MDEA) and anhydride *cis* 4-methyl 1,2,3,6-tetrahydrophtallic (MTHPA) leading to two different chemistries, i.e. polycondensation between amine and epoxyde functions and chain polymerization between epoxyde and anhydride functions. The latter requires the use of an accelerator. A tertiary amine was selected for this purpose, 2,4,6(dimethyl aminomethylene) phenol (DMP30). All reactions for the microbond specimens were conducted for radii epoxyde/anhydride = 1 and epoxyde/amine = 1. The amount of accelerator for the epoxyde/anhydride reaction was set to 1.5 wt%. Chemical formulae, average molar weight and suppliers are presented in Table 4. The chosen radii and the cure schedule (identical to that used for films without pre-cure in Table 5) lead to a fully cross-linked network as revealed by DSC thermograms. Some results are also reported for a DGEBA/diamino diphenyl methane (DDM or MDA) system studied previously [13]. This hardener differs from the MDEA by the presence of the ethylene groups. The DGEBA used in this case shows a polymerization degree of 0.03 (instead of 0.15 for the prepolymer cured with the other hardeners). Glass transition temperatures were measured by differential scanning calorimetry. The Young's modulus and Poisson's ratio used for modelling the experimental data were determined in tension on an Adamel Lhomarghy DY22 apparatus at a cross-head speed of 0.5 mm min^{-1}. The yield point was measured in compression using the same apparatus. The thermal expansion coefficient was determined on a DMA 2980 (TA Instrument) using a penetration clamp at 2°C min^{-1}. Physical and mechanical properties of the cured networks are presented in Table 6.

3.2. Film characterization

Properties of the microdroplets will be characterized

Table 4
Comonomers used in the epoxyde formulations

Name	Formula	Av. molar mass (g mol^{-1})	Supplier
DGEBA $n = 0.15$	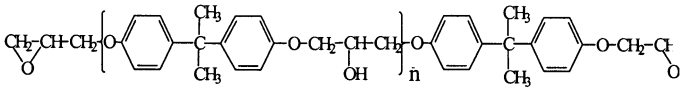	381.2	Ciba Geigy
MDEA	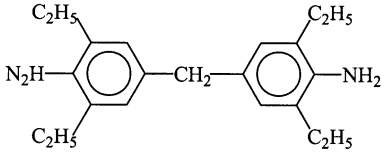	310.5	Lonza
MDA	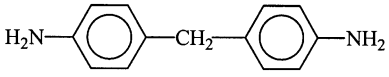	198	Fluka
MTHPA	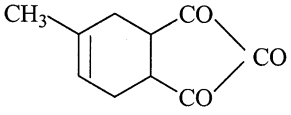	166	Anchor Chemical
DMP30	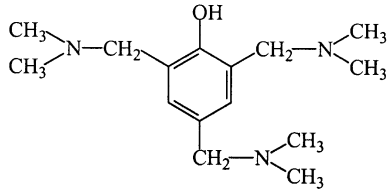	263	Fluka

Table 5
Cure schedule for the preparation of films and bulk samples

Specimens	Hardener	Pre-cure	Cure	Post-cure	Heating rate (°C min^{-1})	Cooling rate (°C min^{-1})
AM0	MDEA	–	4 h, 135°C	4 h, 190°C	2	1
AM48	MDEA	48 h, T_{amb}	4 h, 135°C	4 h, 190°C	2	1
AN0	MTHPA	–	1 h, 100°C	5 h, 160°C	2	1
AN48	MTHPA	48 h, T_{amb}	1 h, 100°C	5 h, 160°C	2	1

through glass temperature transition measurements. For this purpose, we propose the use of thin films, typically from 100 to 200 μm thickness as an ideal microdroplet model. This technique is simple and less time-consuming than the measurement of the glass transition in situ with a cluster of droplets of similar size. It needs only the use of a conventional microcalorimeter and enables infrared analysis to be performed. The films were made by spreading the resin onto an aluminium-covered glass plate using a glass cylinder and subjected to different cure schedules. According to the works of Rao et al. [11], influence of a pre-cure at room temperature was studied. Four kinds of specimen were made, as described in Table 5. A differential scanning calorimeter (Mettler TA 300) was used for glass transition temperature measurements. DSC scans of cured networks as well as thin films were made at 10°C min^{-1} under nitrogen atmosphere using closed pans. The glass transition temperature was estimated from the onset of the transition region. Fourier transform infrared spectroscopy was performed using a Nicolet Magma-IR 550 spectrometer. An Ever-Glo TM source was used along with a KBr bean splitter on a DTGS-KBr detector. The spectra represents a sum of 32 individual scans at 2 cm^{-1} resolution.

3.3. Adhesion measurements

Details concerning specimen preparation and the shearing device can be found in the first part of this paper [9]. Both systems were tested at a cross-head speed of 0.5 mm min^{-1}. In order to assess the visco-elastic behaviour of the specimens, another series of tests was performed at cross-head speeds of 0.05 and 5 mm min^{-1} for the P122 1200 Tex/epoxyde–amine system. Data were fitted by the model of Scheer and Nairn [7] using a classical least-square method. The formalism is briefly presented in Appendix A.

4. Results

4.1. Film properties

For each specimen, two consecutive scans were performed. Typical DSC thermograms for the first and second scans are presented in Fig. 1. In addition to the glass temperature transition region, two other phenomena at high temperature can be observed on the first scan:

(i) some residual exothermy, which can be attributed to the presence of unreacted species;
(ii) an endotherm peak, which can be attributed to the volatilization of unreacted species.

These features are common to specimens AM0 and AN48. For AM48 and AN0, there was only residual exothermy. Since both phenomena are superimposed in two cases, it is not possible to perform a quantitative analysis. Table 7 presents the glass transition temperature for each specimen as well as the temperature from the maximum endotherm peak in comparison with the glass transition temperature of the bulk material. The thickness of the films varied from 100 to 200 μm and was found to have no influence on the measured results. Rao et al. [11] found a dependence of the glass transition temperature when varying the droplet size from 100 to 800 μm, but the value of T_g remains constant in the vicinity of 100 μm, which is in agreement with the results reported there. It should be noticed that for our microbond experiments, the droplet diameter is typically between 50 and 150 μm.

From Table 7, it can be seen that:

(i) films subjected to a pre-cure of 48 h, used as models for our microbond specimens, show a glass transition temperature 50°C lower than that of the bulk material,

Table 6
Mechanical and physical properties of the epoxyde networks

Matrix	T_g (°C)	E (GPa)	ν	Yield stress (MPa)	$\alpha \times 10^4$ (K^{-1})
DGEBA/MDEA	158	3.35	0.41	105.5	1.18
DGEBA/MTHPA	124	3.89	0.37	108.4	0.75
DGEBA/MDA	178	2.90			0.69

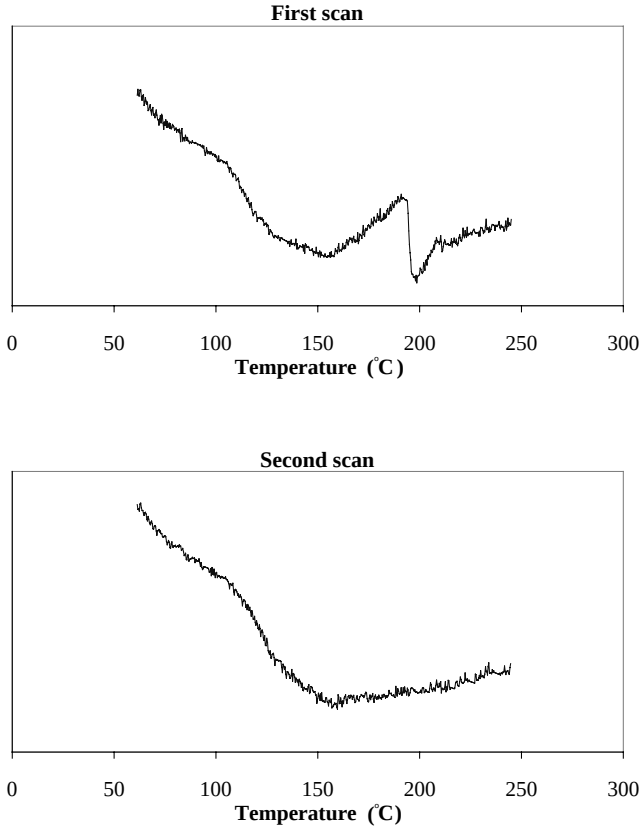

Fig. 1. Typical DSC thermograms for AM0 specimen.

for both epoxyde networks;
(ii) in the case of the polycondensation, the pre-cure has only a small effect on the glass transition temperature;
(iii) in the case of a chain polymerization, the pre-cure at room temperature has a detrimental effect on the droplet properties and should not be performed for the preparation of microbond specimens.

4.2. Interfacial adhesion

Values of the interfacial toughness for the different systems together with the average IFSS are given in Table 8. It can be seen that (i) epoxyde/anhydride microcomposites lead to a stronger interface than the amine-cured network and (ii) the cross-head speed has a great effect on the value of the interfacial toughness as measured by the microbond test. Two typical features of the specimens after testing are presented in Fig. 2, i.e. a cohesive fracture of the polymer and a plastic flow of the microdroplet.

5. Loss in glass transition temperature

The aim of this part is to evaluate the lack of stoichiometry and the consequences on some important materials properties which will in turn affect the stress distribution at the interface and the adhesion between fibre and matrix as measured by the microbond technique.

5.1. Possibles causes

Rao et al. [11] attributed the loss in glass transition temperature to a lack of stoichiometry owing to diffusion and vaporization of the hardener during the cure, the metaphenylenediamine (*m*-PDA). In fact, an improvement was observed after a pre-cure at room temperature which allows the comonomers to react at low temperature and leads to less vaporization. For our systems, this hypothesis cannot explain the totality of the observed phenomena. Indeed, the pre-cure has only a small effect on the amine-based microcomposite, and leads to further loss in glass transition temperature for the epoxyde/anhydride network. Another explanation must be advanced. The fact that the pre-cure does not have the same effect on both systems suggests the occurrence of two different phenomena. We perform an infrared analysis of bulk samples in comparison with films (i.e. microdroplet) in order to obtain information on possible chemical modifications of the network. The spectra for the amine-cured networks are shown in Fig. 3. Two additional bands are observed for the film configuration (i.e. microdroplet). The band at 1661 cm^{-1} is in the proper location to be an imine (C=N), whereas the band at 1723 cm^{-1} is in the range of carbonyl functions (C=O). Culler et al. [14] observed the band at 1661 cm^{-1} on γ-APS after heating the sample above 120°C in air, but it was not present on the spectra after the same treatment under nitrogen atmosphere. They concluded that the primary amines of γ-APS are oxidized to imine groups. The formation of imine groups reduces the number of amine functions that will react with oxirane groups and can explain the loss in T_g observed here. The curing of amine-based microdroplets should thus be performed under inert atmosphere and/or at temperature below 120°C. A simple optical observation on bulk samples cured under the same conditions actually shows an

Table 7
Glass transition temperature and maximum endotherm peak for the film specimens in comparison with bulk material characteristics

Specimens	T_g — first scan (°C)	T_g — second scan (°C)	T — endotherm peak (°C)	T_g — bulk (°C)
AM0	109	115	197	158
AM48	112	111	–	
AN0	104	103	–	124
AN48	69	70	230	

Table 8
IFSS and interfacial toughness for two epoxyde/glass fibre systems tested at different extension rate with microbond technique

Hardener	Cross-speed (mm min^{-1})	G_{ic} Scheer and Nairn (J m^{-2})	Average IFSS (MPa)
MDEA	0.05	32	46 ± 8
MDEA	0.5	189	80 ± 20
MDEA	5	55	52 ± 8
MTHPA	0.5	246	77 ± 14

oxidation coat on the face cured in contact with air. Infrared spectra do not show any additional band for the anhydride system, and no oxidation coat could be observed on the bulk samples. Something else must have happened during the pre-cure, i.e. a phenomenon related to the chemistry of polymerization. The chain polymerization between the epoxyde and anhydride functions can, in fact, be influenced strongly by environmental parameters, such as moisture on fibre surfaces, for instance [15]. It is also known that water hydrolyzes the anhydride hardener leading to the formation of acid functions. This phenomenon could occur during the pre-cure and explain in part the loss in T_g observed here.

5.2. Evaluation of the lack of stoichiometry

Figs. 4–6 present the evolution of the glass transition temperature with respect to the relative proportion of accelerator and comonomers, respectively, for the different bulk systems. It can be seen that losses in T_g due to lack of stoichiometry are more drastic for aromatic diamine than for anhydride, explaining in some parts the differences between specimens AM0 and AN0. The same curve can be found in the literature for an aliphatic Jeffamine [17] and again, the loss in T_g is less important than for the aromatic components, as observed on microbond specimens [11].

The glass transition temperature measured for the film specimens leads to a stoichiometric ratio of 0.8 for specimens AM0, AM48 and AN0 when considering the glass transition of the bulk materials (Figs. 5 and 6). It is more reasonable to consider that epoxyde species are in excess, since (i) there is a possible hydrolysis of the anhydride hardener; (ii) if we consider oxidation, the amine hardener is the affected comonomer; and (iii) it can be seen from bulk materials that specimens with an excess of hardener are more affected by the surface oxidation phenomenon. For the AN48 specimen, this would lead to a ratio of approximately 0.4 under the hypothesis that the anhydride hardener is hydrolyzed during the pre-cure and that acid functions do not react with other functions. The phenol accelerator also plays an important role in this case [16], as shown in Fig. 4 and could also be affected during the pre-cure.

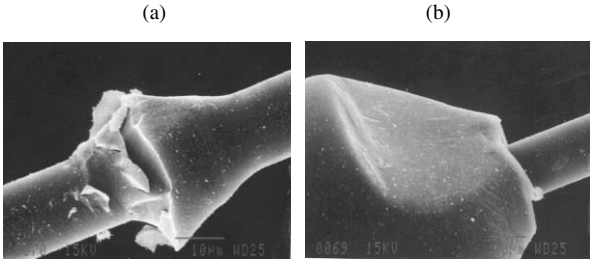

Fig. 2. Post-mortem SEM observations of microbond specimen showing two typical features: (a) the meniscus left on the fibre and (b) the plastic flow of the polymeric droplet. Epoxyde/anhydride/P122 1200 Tex system — cross-head speed 0.5 mm min^{-1}.

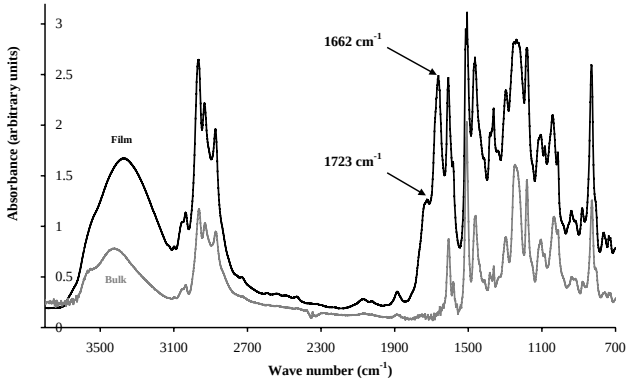

Fig. 3. Infrared spectra of amine-cured epoxyde networks in the film and bulk configuration.

5.3. Consequences

Many material properties are affected by stoichiometry. Among these, the glass transition temperature, tensile and shear modulus, Poisson's ratio and thermal expansion coefficient are of particular interest since they directly affect adhesion at the interface. The yield point will also be discussed briefly since it is related to the plastic flow of the polymeric droplet observed post-mortem.

Evolution of the Young's modulus with respect to the stoichiometric ratio for a DGEBA/MDA system is given in Fig. 7. The modulus presents a maximum at $r = 0.5$ and a minimum at $r = 1$. This has been explained in the

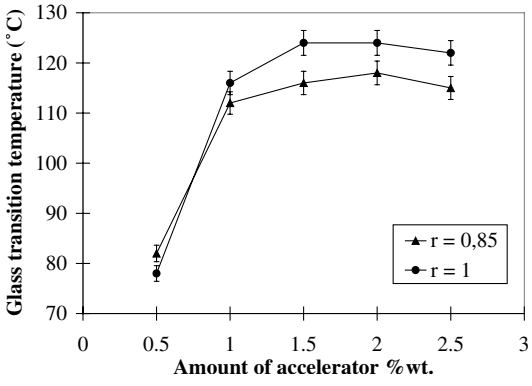

Fig. 4. Evolution of the glass transition temperature with respect to the quantity of accelerator introduced for two anhydride/epoxyde radii.

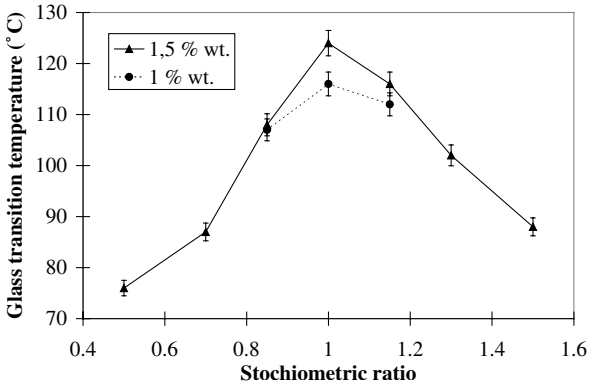

Fig. 5. Evolution of the glass transition temperature with respect to the anhydride/epoxyde ratio for amount of accelerator of 1 and 1.5 wt%.

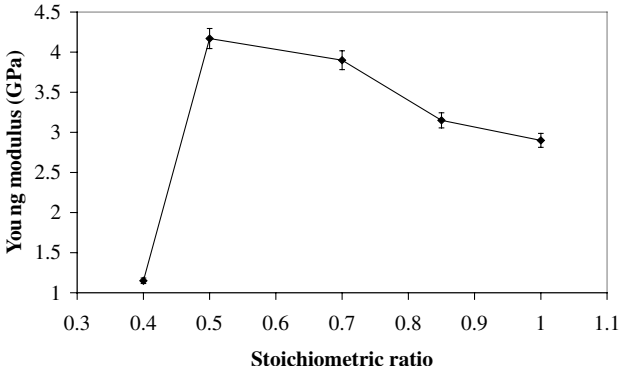

Fig. 7. Evolution of the Young's modulus with respect to the stoichiometric ratio for a DGEBA/MDA system.

literature by an increase in the free volume fraction leading to a lower modulus [18–21]. Other works [17,22–23] observed also a minimum in E in amine-cured epoxyde at the stoichiometric ratio. The lack of stoichiometry leads thus to microdroplets having a higher Young's modulus than the bulk material. This is of great importance since it affects the stress distribution at the interface [24].

The residual shrinking stresses depend on both the glass transition temperature and the thermal expansion ratio α_v in the vitreous state. While the thermal expansion ratio α_c in the rubbery state depends on the relative proportion of comonomers, α_v remains unaffected as shown in Fig. 8 on a DGEBA/MDA system. Thus, we will hereafter assume that internal stresses are only affected by the variation of the glass transition temperature and the Young's modulus.

The yield stress is also affected by the amine/epoxyde ratio [17]. For a DGEBA/polyetheramine, it can decrease from 20 to 30%. This has a direct consequence on the test, since the plastic flow will occur earlier for a microdroplet specimen than for the bulk material.

Variations of shear modulus and Poisson's ratio were not found in the literature. Among the properties affected by the lack of stoichiometry reported here, the influence of the yield stress cannot be treated quantitatively since no model accounts for plastic flow of the polymeric microdroplet. It is nevertheless reasonable to consider that it will lead to an overestimation of the interfacial toughness by dissipating more energy in the flowing process since it will happen at a lower applied load. The effect of glass transition and Young's modulus variations were treated quantitatively with the model of Scheer and Nairn by considering the value of T_g reported in Table 7 for film specimens subjected to a pre-cure. For the amine-cured epoxyde network, the modulus was increased by 10% corresponding approximately to values reported for a stoichiometric ratio of 0.8 (Fig. 7). For the anhydride-based system, the situation is more ambiguous since the loss in modulus occurs in the vicinity of 0.4–0.5. Two corrections are thus proposed, an increase of 10% as well as an intermediate value of 2 GPa. Results are presented in Table 9 for both matrices (0.5 mm min^{-1}). It can be seen that using the properties of the bulk instead of those of the microdroplets leads to (i) an underestimation of the interfacial toughness by considering a greater amount of residual stresses and (ii) an overestimation of G_{ic} by considering a biased value of the modulus in the case of the epoxyde amine matrix. Since the former is more important, the sum of both effects results in an 'effective' interfacial toughness (note that Poisson's ratio, the shear modulus and the yield stress/plastic flow

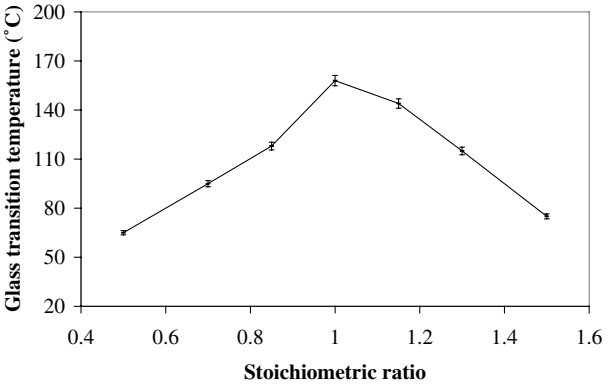

Fig. 6. Evolution of the glass transition temperature with respect to the amine/epoxyde for two different aromatic diamines, MDA and MDEA.

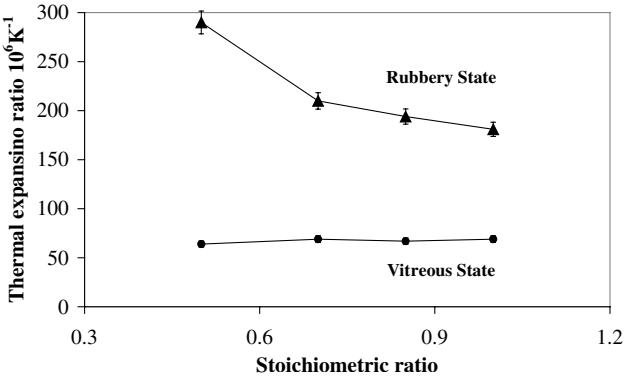

Fig. 8. Evolution of the thermal expansion coefficient with respect to the stoichiometric ratio for a DGEBA/MDA system.

Table 9
Corrections proposed on the interfacial toughness due to specific properties of the microdroplet

Hardener	Correction	G_{ic} Scheer and Nairn (J m^{-2})
MDEA	Bulk conditions	189
MDEA	E + 10%	169
MDEA	ΔT	237
MDEA	ΔT, E	217
MTHPA	Bulk conditions	246
MTHPA	E + 10%	230
MTHPA	E 2 GPa	415
MTHPA	ΔT	278
MTHPA	ΔT, E + 10%	261
MTHPA	ΔT, E 2 GPa	449

have not been considered yet) greater than that observed when using bulk material properties. When the microbond test is performed in an attempt to compare different sizing and/or surface treatments, the relative trends will remain the same if the same matrix is used. When comparing different matrices, this error can lead to biased results since the value of the ΔT correction can differ significantly according to the type of matrix used (see AM0 and AN0 in Table 7 as an example).

6. On the non-elastic behaviour of microcomposites

6.1. Dissipative systems?

The microbond specimen can be considered to be made of three components, i.e. the fibre, interphase and matrix. The fibre can be considered as an ideal elastic component. As shown in Fig. 2, the matrix undergoes plastic deformation and cannot be considered as an ideal elastic component. It is thus important to know whether the observed plastic flow of the polymeric microdroplet is specific to our systems or inherent to the microbond testing. It can be explained only in some part by the loss in yield stress owing to the lack of stoichiometry since it was also observed with a thermoplastic matrix [10]. If we consider the surface of deformation from the SEM picture (Fig. 2 — from 500 to 1000 μm^2, approximately) and the maximum applied load between 0.5 and 1 N, the local stress ranges from 0.5 to 2 GPa. Those values are several times greater than the yield stress of the bulk material (Table 5). When droplets are formed on the fibre, they conform to its cylindrical shape but, depending on the contact angle and volume of the droplet, a meniscus will always exist at the contact point of the fibre and matrix [25–27]. At the beginning of the test, the area of contact between the microvice and the droplet is very small, resulting in a very high local applied stress. The yield point can be reached locally, and if the maximum applied load is high enough, the local plastic deformation can explain the SEM photographs in Fig. 2.

The plastic flow of the polymeric microdroplet is thus probably inherent to the microbond technique, and even more important in the case of certain epoxyde matrices showing a lack of stoichiometry. When a polymer is deformed in the glassy state, three components of its deformation are distinguished [28–31]: elastic, visco-elastic and plastic deformation. The elastic strain recovers instantaneously, the visco-elastic recovers over a large range of time, and the plastic one is permanent. Girard-Reydet et al. [28] showed for a DGEBA/4,4′-methylenebis3-chloro 2,6-diethylaniline (MCDEA) system that the visco-elastic contribution is preponderant. In their experiments, while the total deformation was set to 18%, the visco-elastic part measured after a recovery of 30 min represented 11%, more than one half of the total strain. It means that the deformation occurring during the microbond experiment is even more important than that observed on SEM photographs that were taken a few days after the test.

An important consequence concerns the idealized specimen used for theoretical works. Models dealing with the classical pull-out configuration cannot account for this non-elastic process since the load is generally considered to be applied uniformly. Scheer and Nairn also made this assumption, by considering a cylinder on the fibre instead of an ellipsoidal droplet. New theoretical analyses have to be developed using idealized specimens that enable us to account for the plastic flow. The use of the J integral, which is a better criterion for dissipative systems than G [32], can be envisaged.

6.2. Evidence of rate-dependent processes

The only study in the literature dealing with the influence of the extension rate on the microbond results was conducted on a Kevlar/epoxyde system [33]. The cross-head speed was varied over two orders of magnitude, and a slight increase (<10%) in the measured average IFSS was found. The results reported here, however, show a drastic influence of the loading rate. We have to recognize that the variations of the interfacial toughness versus loading rate remain unsolved, yet some hypotheses can be advanced. Changes of fracture behaviour can be observed with changing loading rate, and especially for glassy polymers having a low shear yield stress [32]. At a cross-speed of 0.05 mm min^{-1}, there was evidence of ductile fracture of the interface. While the extension rate increases, specimens give a brittle fracture. Both visco-elastic and plastic contributions on the matrix deformation depend on the loading rate. The structure of the interphase generated by the presence of an alkoxysilane coupling agent gives a continuum from the glass surface — reacted silanols — to the polysiloxane/matrix interpenetrated network [34]. The exact location of the failure is not yet known, and could vary with varying loading rate. The particular structure of the interface layers, close to those obtained from the sol–gel chemistry of hybrids [35] can lead to specific energy absorption

processes. It is possible that rate-dependent processes cease to operate at some loading rate level, similar to crazing in the fracture of thermoplastics, for instance [32].

7. Concluding remarks

The physical and mechanical properties of microdroplets can differ significantly from those of the bulk material. This is especially true for epoxyde droplets, owing to (i) diffusion and vaporization of the hardener during the first step of the cure, (ii) surface oxidation and (iii) possible hydrolysis of the hardener during the first step of the cure schedule. The glass transition temperature of microdroplets was found to be 20–50°C lower than that of the bulk material. It is shown that this leads to microdroplets exhibiting a higher Young's modulus and a lower yield point than the bulk network. Those discrepancies influence the adhesion between fibre and matrix by changing the stress distribution at the interface and can lead to biased results when comparing different matrices with the microbond test. The general idea that microbond specimens behave like ideal elastic components is now reassessed in view of (i) a plastic flow of the polymeric droplet and (ii) the occurrence of rate-dependent processes. This leads to a fundamental question regarding the use of microcomposites as a model of macroscopic-scale specimens.

Acknowledgements

We want to thank DER/EDF for its financial support. The French Embassy of Israel in Tel-Aviv is gratefully acknowledged for providing grants under the 'Arc-en-Ciel–Keshet' program in order to enhance the scientific exchanges between LMM/INSA and the Weizmann Institute (Department of Materials and Interfaces).

Appendix A. Theoretical analysis from Scheer and Nairn

The simplified analysis derived from variational mechanics leads to

$$\sigma_d(\rho) = -\frac{D_{3s}\Delta T}{C_{33s}} + \sqrt{\frac{2G_{ic}}{r_f C_{33s}} + \frac{\Delta T^2}{C_{33s}}\left(\frac{D_{3s}^2}{C_{33s}} - \frac{D_3^2}{C_{33}}\right)}$$

where σ_d is the stress at decohesion and ρ the axial ratio (embedded length/fibre diameter), r_f the fibre radius, ΔT the difference between the stress-free temperature and the room temperature, the C and D constants depend on the sample dimensions and on the mechanical properties of the fibre and the matrix:

$$C_{33s} = \frac{1}{2}\left(\frac{1}{E_F} + \frac{V_f}{V_m E_m}\right)$$

$$D_{3s} = \tfrac{1}{2}(\alpha_f - \alpha_m)$$

$$C_{33} = \frac{1}{2}\left(\frac{1}{E_F} + \frac{V_f}{V_m E_m}\right) - \frac{V_m A_3^2}{V_f A_0}$$

$$D_3 = -\frac{V_m A_3}{V_f A_0}[\alpha_T - \alpha_m] + \frac{1}{2}(\alpha_f - \alpha_m)$$

$$A_0 = \frac{V_m(1-\nu_T)}{V_f E_T} + \frac{1-\nu_m}{E_m} + \frac{1+\nu_m}{V_f E_m}$$

$$A_3 = -\left(\frac{\nu_f}{E_f} + \frac{V_f \nu_m}{V_m E_m}\right)$$

In these equations, E_f and E_T are the axial and transverse tensile moduli of the fibre, ν_f and ν_T the axial and transverse Poisson's ratio of the fibre, α_f and α_T the axial and transverse thermal expansion coefficients of the fibre, E_m, ν_m and α_m the tensile modulus, Poisson's ratio and thermal expansion coefficient of the matrix. V_f and V_m are the volume fraction of the fibre and the matrix, respectively. According to the works of Scheer and Nairn, they were calculated from the plot measured droplet diameter versus measured droplet length.

References

[1] Koenig JL, Emadipour H. Polym Compos 1985;6(3):142.
[2] Zinck P, Lacrampe V, Gérard JF. Rev Compos Mater Avances 1997;7:31.
[3] Ahlstrom C. PhD thesis, INSA de Lyon, 1988.
[4] Desaeger M, Verpoest I. Compos Sci Technol 1993;48:215.
[5] DiFrancia C, Ward TC, Claus RO. Composites 1996;27A:597.
[6] Miller B, Muri P, Rebenfeld L. Compos Sci Technol 1987;28:17.
[7] Scheer RJ, Nairn JA. J Adhesion 1995;53:45.
[8] Marotzke C, Hampe A. Proceedings of ICCM-10, Whistler, Canada VI-517, 1995.
[9] Zinck P, Wagner HD, Salmon L, Gérard JF. Submitted for publication.
[10] Gonon L, Momtaz A, Van Hoyweghen D, Chabert B, Gérard JF, Gaertner R. Polym Compos 1996;17:265.
[11] Rao V, Herrera-Franco P, Ozzello AD, Drzal LT. J Adhesion 1991;34:65.
[12] Biro DA, McLean P, Deslandes Y. Polym Engng Sci 1991;37(17):1250.
[13] Perret P. PhD thesis, INSA de Lyon, 1988.
[14] Culler SR, Ishida H, Koenig JL. Polym Compos 1986;7(4):231.
[15] Van Mele B, Verdonck E. Compos Int 1995;3(2):101.
[16] Urbaczewski E. PhD thesis, INSA de Lyon, 1989.
[17] Morgan RJ, Kong FM, Walkup CM. Polymer 1984;25:375.
[18] Takahama T, Geil PH. J Polym Sci Polym Phys Ed 1982;20:1979.
[19] Gupta VB, Drzal LT, Lee CYC, Rich MJ. J Macromol Sci Phys B 1984–1985;23:435.
[20] Gupta VB, Drzal LT, Lee CYC, Rich MJ. Polym Engng Sci 1985;25(13):812.
[21] Enns JB, Gillham JK. J Appl Polym Sci 1983;28:2831.
[22] Selby K, Miller LE. J Mater Sci 1975;10:12.
[23] Kim SL, Skibo MD, Manson JA, Hertzberg RW, Janiszewski J. J Polym Engng Sci 1978;18:1093.
[24] Venkatakrishnaiah S, Dharani LR. Eur J Mech A Solids 1994;13(3):311.

[25] Herrera-Franco PJ, Drzal LT. Composites 1992;23:2.
[26] Wagner HD. J Appl Phys 1990;67(3):1352.
[27] Carrol BJ. Langmuir 1986;2:248.
[28] Girard-Reydet E, Vicard V, Pascault JP, Sautereau H. J Appl Polym Sci 1997;65:2433.
[29] Quinson R, Perrez J, Rink M, Pavan A. J Mater Sci 2001 (in press).
[30] Oleynick E. Prog Colloid Polym Sci 1989;80:140.
[31] Oleynick E. In: Baer X, editor. High performance polymers. Munich, 1990. p. 79.
[32] Williams JG. Fracture mechanics of polymers. Chichester, UK: Ellis Horwood, 1984.
[33] Gaur U, Miller B. Compos Sci Technol 1989;34:35.
[34] Jones FR. Key Engng Mater 1996;116–117:41.
[35] Zinck P, Pays MF, Rezakhanlou R, Gérard JF. J Mater Sci 1998;33:1.